JOURNAL OF THERMOPHYSICS AND HEAT TRANSFER
Vol. 17, No. 4, October–December 2003

Determination of Reflectance Function for Aluminum and Stainless-Steel Foil Surfaces

Mauricio A. Sanchez* and William H. Sutton†
University of Oklahoma, Norman, Oklahoma 73019

A Kirchhoff-based relationship and a Rayleigh–Rice perturbation theory were two evaluated analytical methods used to account for the reflectance function determination in rough metallic surfaces. These methods proved to be inconclusive at predicting reflectance function in rough surfaces due to the inability to handle all the dependencies a rough reflector possesses with respect to an incoming incident energy ray (intensity, magnitude, wavelength) and surface characterization (rms roughness and slope, power spectral density). Experimental determination was shown to be the best method to attain directional properties. An experimental scatterometer based on the angular discretization of the discrete ordinates or S_N method was used and tested to measure surface reflectance. Results obtained could be easily applied to radiative heat transfer calculations, radiative property determination, and surface finish parameters in manufacturing applications.

Nomenclature

f	=	spatial frequency
I	=	intensity of radiation
L	=	observation length of the surface or characteristic length
lc	=	autocorrelation length
m	=	rms surface slope
R	=	Fresnel intensity reflection coefficients
r	=	direction
$S_2(\boldsymbol{f})$	=	power spectral density
$\hat{s}_i$	=	directions of quadrature
x, y, z	=	Cartesian coordinates
Θ	=	polar angle
λ	=	wavelength
ρ	=	reflectance or reflectance function
σ	=	rms surface roughness
Φ	=	azimuthal angle
Ω	=	directional angle, solid angle
ϖ_i	=	quadrature weights

Subscripts

i	=	incident
o	=	optical
s	=	scattered

Superscripts

d	=	diffuse
s	=	specular
‘	=	incoming or incident

I. Introduction

EXACT definitions of the radiative surface properties can be found in the literature.[1–3] However, a brief account will be given of directional radiative properties that play an important role in the solution of radiation transfer problems for optical or energy scattering.

The most important radiative property, which describes the scattering of radiation from a surface, is known as the reflectance function. This function is required to completely describe the radiative characteristics of any surface because all other property functions are related to it and it may also determine the intensity distribution in the scattered flux if the intensity distribution of the incident energy previously known.

The reflectance function is denoted as $\rho_\lambda(\Theta_i, \Phi_i, \Theta_s, \Phi_s)$ and has units of inverse steradians. When the function is multiplied by the incident intensity $I_\lambda(\Theta_i, \Phi_i)$, the cosine of the polar angle $\cos(\Theta_i)$, which the incident intensity makes with the normal of the surface (Fig. 1), and the solid angle $d\Omega = \sin(\Theta)\, d\Theta\, d\Phi$, and finally all integrated over the hemisphere bounded by the surface, the result originates in the reflected intensity in the directions (Θ_s, Φ_s) (Ref. 1)

$$I_\lambda(\Theta_s, \Phi_s) = \frac{1}{\pi} \int_{4\pi} I_\lambda(\Theta_i, \Phi_i)\rho_\lambda(\Theta_i, \Phi_i, \Theta_s, \Phi_s) \times \cos(\Phi_i)\sin(\Theta_i)\, d\Theta_i\, d\Phi_i \tag{1}$$

where Θ_s and Θ_i are the scattered and incident polar angles and $d\Omega$ is the solid angle defined as the projection of the surface onto a plane normal to the direction vector divided by the distance squared, as illustrated in Fig. 1.

There are numerous ways in which the reflectance function can be obtained, but all of them are based on the surface finish of the reflector. For instance, in geometric optics, a ray trace of the energy incident on the rough surface as it leaves,[4] assuming a Fresnel reflection from a locally optically smooth surface, may be used. This function, also known as the bidirectional reflection distribution function (BRDF), is usually predicted for smooth surfaces by surface profile measurements plus information about the statistical symmetry of the surface reflector.[5] However, the best way to attain the function is by experimentation, because this provides the correct information from a surface reflector.

The necessity of reliable data on scattering from the solid materials is growing continually. Frequently, existing data on directional properties cannot be used accurately unless some simplifying assumptions are made. Therefore, in many cases there is a need to correct and enhance these values, which allows for proper use of existing numerical models. Again, this can be done by measurement of that given property.

Many of the scattering and reflecting characteristics of surfaces have been based on relating a profile measurement with the theory of electromagnetic waves reflection. One of the first pioneers in this field was Davies,[6] who studied the scattering of radar waves from rough water surfaces. This was fully enhanced by H. E. Bennet and

Received 7 March 2003; revision received 23 May 2003; accepted for publication 27 May 2003.

*Research Assistant, School of Aerospace and Mechanical Engineering, 865 Asp Avenue, Room 121. Member AIAA.

†Professor, School of Aerospace and Mechanical Engineering, 865 Asp Avenue, Room 208. Member AIAA.

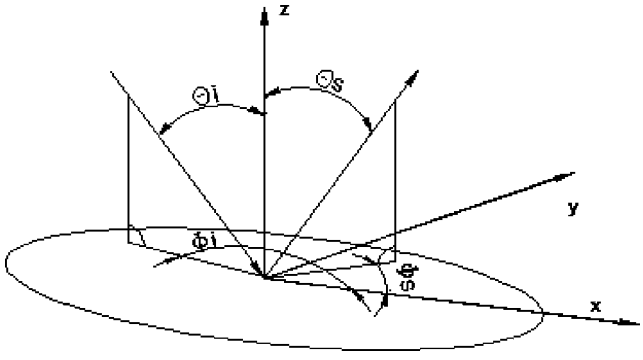

Fig. 1 Surface reflector coordinate system.

J. O. Porteus,[7] who measured the scattered power from a surface and then normalized it to the reflected specular power. The ratio is defined as the total integrated scatter (TIS).[6] Although the TIS development can be used as a source to measure the rms roughness σ (or Rq) of a surface as a true measure of the two-dimensional area it fails to describe the true scattering properties of the reflector. For instance, it can only be used for angles close to normal incidence. It also assumes that the specular angle is the same as the incident angle and that a surface has a Gaussian height distribution function. Finally, TIS neither accounts for polarization effects, nor can it be used for reliable comparison with other profiling instruments.

Beckmann and Spizzinno[8] gave a more complete approach, in which they made use of the Kirchhoff-based relationship to derive the function for isotropic surfaces with a normal Gaussian height distribution. After Bennet and Porteous,[7] Beckmann used an expression called the autocovariance length or autocorrelation function $lc = \sigma\sqrt{(2)}/m$. This function included the rms slope m (or Rdq) to give a more complete detail of the surface profile.

By 1965 similar work by Birkebak and Eckert[9] demonstrated the use of the work done by Bennet and Porteus[7] by conducting a series of experiments (using gonioreflectometers) and analysis (using electromagnetic theory correlations) in which the reflectance function was determined. At the same time Torrance and Sparrow[10] made use of the geometric optics concepts (including masking and shadowing) to account for the reflectance function in comparison with previous goniometric experimentation. Their numerical results agreed well with the experimental values for the different surface reflectors.

Although an off-specular shifting phenomenon has been evident in published reflectance data, but not fully reported due to the way the data was plotted, Torrance and Sparrow,[10] and later Love and Francis,[11] provided a glimpse of this particular phenomenon in the experiments conducted using rough metallic and nonmetallic surfaces for unpolarized incident radiation. This phenomenon appears when the size of surface features is greater than the incident wavelength: $(\sigma/\lambda) > 1$. Torrance and Sparrow created a model using geometric optics to describe reflectance for very rough surfaces. Smith et al.[12] detailed a new characteristic of the off-specular shifting phenomena (termed subspecular and superspecular) while measuring polarized radiant flux reflected from roughened glass samples. Their geometric optics analysis, which account for the s- and p-type polarization, agrees very well with the experimental data for small angles of incidence.

Houchens and Hering[13] compared the Davies[6] and Beckman–Spizzinno[8] models. Both of these models work by separating the specular energy component and the diffuse component of the reflectance through the use of the optical roughness (σ/λ) and autocorrelation roughness parameters (lc/λ). It has been demonstrated that the Beckman–Spizzinno model was more accurate than the Davies model; however, both of these models fail to give an exact value of the reflectance because many different values of roughness and autocorrelation lengths can result in the same values of reflectance.[3]

It is interesting to note that the aforementioned models use at least two profile measures (σ, m) to come up with the reflectance for roughened reflectors. Different models have also arisen for surfaces in the limit of slightly rough surfaces and for perfectly smooth surfaces using profilometry. Except for the case of a perfectly smooth surface (no surface profile needed), the surface scattering is all in the specular direction and the reflectance function can be found using the Fresnel theory.

For modeling a slightly rough surface, the reflectance function consists of a specular component and a reduced diffuse component, which is principally in off-specular directions. This function can still be found using the TIS formulation but it now includes the diminished specular scatter and the diffuse scatter. In the case of a slightly rough surface made of a perfectly conducting material the sum of the specular and diffuse scatter equals one (and the emissivity is zero). In the case of a slightly rough non-perfectly conducting material the sum of the specular and diffuse components is less than one (and the emissivity is nonvanishing). That is, there are nonvanishing effects of the surface roughness.

If the surface reflector is in the limit of a slightly rough surface, where $(4\pi\sigma/\lambda)^2 \ll 1$, then both the specular and diffuse surface scatter and the TIS can be expressed in terms of the two-dimensional power spectral density (PSD) of the surface roughness. The PSD can be found through the use of Fourier analysis and random signal theory from profile measurements (perturbation theory).

There are important issues involving the smooth-perturbation results. For instance, many surfaces are fractal-like in that their PSD increases rather than levels off at low spatial frequencies. Thus, the evaluation of the rms roughness from real surface measurements is uncertain, because real surface measurements give information only down to the nonvanishing frequency on the PSD, $1/L$, where L is the observation length on the surface.

Extensive published literature about reflectance function prediction for smooth surfaces that possess some microroughness has been available since the late 1970s. John Stover[3] provided an excellent treatise about optical scattering and reflectance function predictions through the use of PSD.

When the surface is rougher than permitted by the smooth-surface requirement, meaning that the surface features are larger than the radiation wavelength, other approaches can be taken for the reflectance function determination. As pointed out previously, geometric optics is a method that has been used with success to determine biangular reflectance in very rough surfaces.[4,10,12,14] However, for surfaces that are less than very rough, with concentrated anisotropy in their profile, a common method to predict reflectance is by conducting light-scattering experiments. Experimentation can capture the reflectance function of any surface; the data extracted from it can be used not only for surface profilometry and surface defect detection but also as a tool for computer graphics and image-based processes. Germer[15,16] used the polarization of scattered light to account for the information that can be used to establish the source of the scatter and localize local defects especially in smooth surfaces. For instance, Marschner et al.[17] showed that the main point of computer graphics and image-based measurements is to analyze the photographic data, pixel by pixel, of a three-dimensional object around the hemisphere and convert it into reflectance data by normalizing it with the irradiance of the source.

It can be stated that a spectral reflectance function (because it is also dependent on the wavelength of the radiation) can be predicted in several ways. Most commonly it is obtained from surface profile measurements (optical or mechanical), plus information about the symmetry of the surface adding a reflection theory (Kirchhoff, perturbation, geometric optics, etc.), knowing that the function from one wavelength to another is model dependent. But, direct reflectance measurements are more sensitive to the effects of surface defects than any other profile-based method.

The following sections will provide with the analysis and experimental results to account for the spectral or wavelength region-dependent reflectance function in two metallic materials that comprised a fire-layered barrier.[18] Description of the parameters and formulas is provided along with the experimental results from the calibrated systems.

The American Society of Testing Material (ASTM) provides a calibration scheme and methodology for relating the reflected

and incident intensities in reflectance measurements from an opaque surface.[19] Some experimental results here are calibrated through National Institute of Standards and Technology (NIST) standards, whereas others are derived through light-scattering experiments done on a rough gold surface at different angles of incidence taking into account the ASTM relative measurement methodology. The results provide another means to compare simple analytical predictions of surface scattering with experimental data.

II. Theory

The current work was done to support the analysis of directional properties in layered fire barrier materials, which are often fabricated with alternating layers of foil and fibrous insulation. Available results for reflectance function for these foils are limited in the open literature, except for published values of hemispherical reflectance made to materials of the same chemical characteristics but of unknown surface morphology.

Radiation heat transfer through to the foil and insulation materials accounts for almost 60% of the heat transfer in fire barriers; the rest is due to conduction and convection. Because this radiation heat transfer is such an influential factor, the radiative properties of both materials (metal and insulation) are determined. Here we will consider measurements with two different light sources covering measurements at 0.638 μm and 2 thermal/wavelength ranges in the infrared region (2–20 μm) for the directional reflectance distribution of the foils.

The main purpose of the foil layer is to reflect thermal radiation. To accomplish that, a highly reflective material would work best. Aluminum foil is a good candidate because it is highly reflective, but it cannot withstand the high fireside temperatures. Stainless-steel foil can also be used in conjunction with the aluminum because this material can be positioned at the outer layers of the multilayer fire barrier to withstand the direct temperatures involved in the fire. The foil materials chosen for this study are heavy-gauge aluminum foil, type 303-H14, 0.406 mm thick and corrosion resistant, and stainless-steel foil, type 321, 0.102 mm thick and corrosion resistant.

Based on the discussion, two attempts were evaluated to determine the reflectance function $\rho_\lambda(\theta_i, \Phi_i; \theta_s, \Phi_s)$ for the metallic materials. Kirchhoff-based relationships using the Beckmann and Spizzinno models and the formulation for the slightly rough surface models were used because the criterion for smoothness is often quoted as $\sigma < \lambda/20$, where λ is the wavelength of the incident radiation, so that the metallic foils will have a reflectance characteristic that approaches that of an ideal specular reflector. Only this method considers polarization effects of the reflected light.

To make use of any of the preceding models, surface profilometry must be performed to determine the characteristics of the reflector. Three surface parameters must be considered for the aforementioned models: the rms surface roughness σ (or Rq), the rms surface slope m (or Rdq) for the first model, and the two-dimensional PSD for the second one. The PSD can be considered a surface roughness power per unit spatial frequency. Moreover, the rms surface roughness is the square root of the integral of the PSD (the zeroth moment) and the rms slope is given by the square root of the second moment.[3] A more detailed definition of surface parameters can be defined and calculated from profile data[3] and in the literature.[19,20] The Kirchhoff-based relationships using the Beckmann–Spizzinno model[3] state that the surface must be an isotropic random rough reflector with a Gaussian height distribution and autocorrelation function lc. This formulation results in six cases that cover smooth, general, and rough surface calculations for both one- and two-dimensional reflectors. (The scattering surface is considered two-dimensional such that spatial frequencies, which propagate in two directions, are necessary to represent surface and scatter pattern.[3]) Beckmann's two-dimensional rough surface reflectance function can be expressed as

$$\rho(\Theta_i, \Phi_i; \Theta_s, \Phi_s) = \pi R(\Theta_i) F_3^2 (L/\lambda) \exp -(\pi f L)^2 \qquad (2)$$

with

$$F_3 = \frac{1 + \cos(\Theta_i)\cos(\Theta_s) - \sin(\Theta_i)\sin(\Phi_s)}{\cos(\theta_i)[\cos(\Theta_i) + \cos(\Theta_s)]}$$

$$f = \frac{1}{\lambda}\left\{[\sin(\Theta_i)\cos(\Phi_s) - \sin(\Theta_i)]^2 + [\sin(\Theta_s)\sin(\Phi_s)]^2\right\}^{\frac{1}{2}}$$

$$L = \frac{lc\lambda}{2\pi\sigma[\cos(\Theta_i) + \cos(\Theta_s)]}$$

where R is a Fresnel factor, F_3 is an obliquity factor, f is the spatial frequency, and L is a characteristic length. Because the terms σ and lc appear in Eq. (2) as a ratio, $\sqrt{(2)}\sigma/lc$, they become a single variable called rms slope.

The Rayleigh–Rice perturbation theory,[3] which describes the reflectance function for reflectors in slightly rough or smooth surfaces is given as

$$\rho(\Theta_i, \Phi_i; \Theta_s, \Phi_s) = (16\pi^2/\lambda^4)\cos(\Theta_i)\cos(\Theta_s)\sqrt{R(\Theta_i)R(\Theta_s)}S_2(f) \qquad (3)$$

where the angles Θ and Φ follow the description of Fig. 1, the R terms are the Fresnel intensity reflection coefficients, the factor S_2 is the PSD, which contains information about the surface roughness, and f represents surface frequency of the spectrum. Its components in the surface plane are in relation to the reflection parameters by the following grating equations[20]:

$$f_x = \frac{1}{\lambda}[\sin(\Theta_s)\cos(\Phi_s) - \sin(\Theta_i)]$$

$$f_y = \frac{1}{\lambda}[\sin(\Theta_s)\sin(\Phi_s)] \qquad (4)$$

Equations 3 and 4 originate from derivations of the vector perturbation theory with regard to topographic reflection. Converting height fluctuations into phase fluctuations gives Eq. (3). As a result, the near-field phase fluctuations can be extended into a far-field intensity distribution.[20]

III. Validation

To validate Eq. (1) with the metallic surfaces composing the fire barrier, surface profilometry must be executed prior solving for the reflectance function.

Figure 2 shows the filtered surface profiles (according to ISO 11562) of one of the four aluminum and stainless-steel samples using data collected by a Taylor Hubson® surface profilometer located at the Surface Metrology Lab at the Center for Precision Metrology in the Department of Mechanical Engineering and

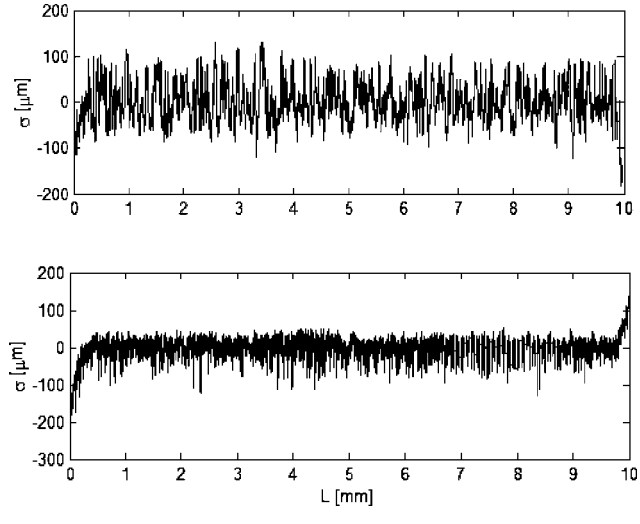

Fig. 2 Filtered roughness profile of aluminum (up) and stainless-steel foils (spacing between points 0.25 μm, cutoff 0.8 mm; courtesy of UNCC Dimensional Metrology Laboratory).

Table 1 Average surface profile data of metallic foils

Surface parameter	Aluminum	SS 321
σ, Rq, μm	0.4484 ± 0.0099	0.2140 ± 0.003
rms Slope m, Rdq, deg	4.5120 ± 0.1150	6.2013 ± 0.090

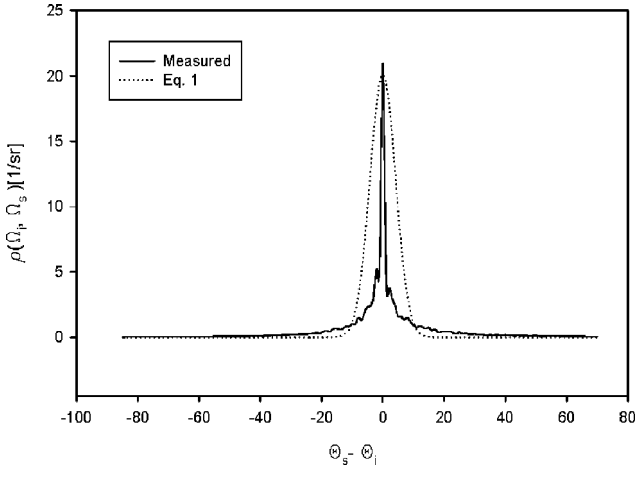

Fig. 3 Reflectance of stainless-steel foil ($\Theta_i = 15$ deg, $\Phi_s = \Phi_i = 0$ deg, $lc = 6.231$; courtesy of NIST Bidirectional Optical Scattering Facility).

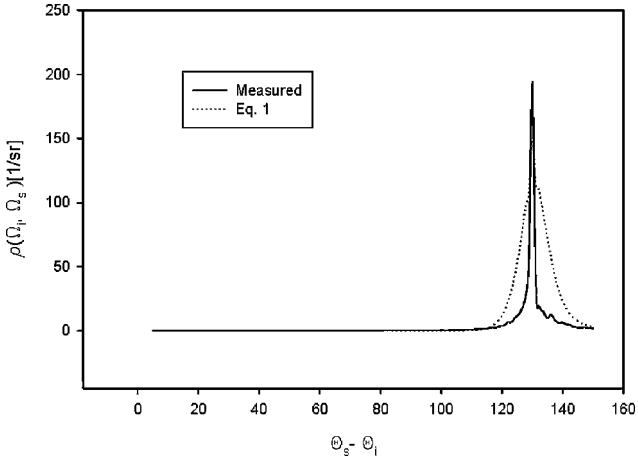

Fig. 4 Reflectance of stainless-steel foil ($\Theta_i = 60$ deg, $\Phi_s = \Phi_i = 0$ deg, $lc = 6.231$; courtesy of NIST Bidirectional Optical Scattering Facility).

Engineering Science, University of North Carolina–Charlotte. Table 1 lists the average surface profile data of the samples.

As seen in the figure and table, the aluminum has almost twice the roughness of the stainless steel. It is to be expected that the stainless foil would have a much more specular scattering behavior than the aluminum material for certain wavelength ranges.

Prior to examining scattering effects for the foils in the infrared region, experimental measurements of the reflectance function were performed using a goniometric optical scatter instrument at the Bidirectional Optical Scattering Facility at NIST, Gaithersburg, Maryland.

In-plane measurements at 15, 40, and 65 deg and out-of-plane measurements with incident and scattering angles equal to 65 deg were carried out. All of the data represent the unpolarized reflectance function at 0.633 μm. All measurements were performed for six different equally spaced sample rotations (sum of Φ_s and Φ_i from 0 to 150 deg).

Figures 3 and 4 show the reflectance function found by Eq. (1) in comparison to the experimental data. For these measurements several caveats are generated. First, a full uncertainty analysis was not performed for the scattering data. Second, although the systematic uncertainties are typically less than 1% of the signal, the signal noise is typically dominated by laser speckle, which can be estimated by the apparent point-to-point fluctuations in the data. Finally, the alignment of the sample surface, made difficult by the lack of sample rigidity, created a large (few degrees) uncertainty in the incident and scattering angles. It can be noticed that the reflectance obtained by Eq. (2) is not accurate because it was made for isotropic and Gaussian surfaces, something that does not correspond to the actual surfaces of the foils (at least the aluminum foil) because they present anisotropy in surface profile (to be demonstrated later).

There seems to be no relation between the rms slope m measured by the profilometer and the rms slope derived by the equation. Values of autocorrelation length were estimated to obtain a close fit to the data because the use of the rms slope to obtain the autocorrelation function provided a very poor reflectance function profile. Moreover, as pointed out by Houchens and Hering[13] and Stover,[3] the ratio σ/lc, obtained by many values of the rms roughness and autocorrelation lengths, will produce the same reflectance. Houchens and Hering also questioned the value of lc because it should be a constant parameter for all wavelengths of radiation, something that did not occur in the measurements conducted in the literature.

Because these reflectance measurements fall into the category of measurements from opaque optics, they can be used to estimate the optical rms roughness σ_o by making use of the TIS approach. Scalar reflection theory[3] related the measured TIS to the rms surface roughness σ:

$$\mathrm{TIS} = [4\pi\sigma \cos(\Theta_i)/\lambda]^2 \tag{5}$$

Equation 5 can only be used for angles close to normal incidence. It also assumes that the specular angle is the same as the incident angle, the surface has a Gaussian height distribution function, and σ is assumed to be smaller than λ. Finally, TIS neither accounts for polarization effects nor can it be used for comparison with other profiling instruments. By assuming that the surfaces are normally distributed and by taking the specular component of the reflectance function for an angle of incidence of 15 deg, the optical rms roughness σ_o is 0.414 μm for the aluminum foil sample and 0.302 μm for the stainless-steel foil sample, which agrees well with the profilometer data.

As previously indicated, the aforementioned observations showed that when the angle of incidence is increased, the specular response of the roughened material increases. The same results also show an apparent off-specular shifting[10–12] where the specular reflected peak occurs at some leaving direction other than the specular direction, as predicted by Fresnel equations. This shifting becomes more pronounced as the surface roughness or the anisotropy of the surface increases at a given wavelength: $(\sigma/\lambda) \geq 1$. For these metallic foils, the apparent off-specular shifting is more pronounced for the aluminum foil than for the much less rough stainless-steel foil because at the measured wavelength of incidence (0.633 μm) the shifting is more accentuated for rougher surfaces. However, this phenomenon is not greatly pronounced because these metallic surfaces visually have a mirror-like appearance. This apparent shifting (Fig. 5) is simply due to the range of the uncertainty of the measured angles, which corresponds to the change of the specular scattering angle for the respective foils (1 or 2 deg for the steel and the aluminum, respectively), and it is too small to be shown in the scale of the figure.

If the magnitude of the surface anisotropy is sufficiently large (compared to the energy incident wavelength), the off-specular shifting occurs, which might be used as a reference parameter to describe its surface properties. As the angle of incidence increases, the surface becomes very specular and surface roughness and/or wavelengths effects are minimized.

For the far-infrared region, the surfaces reach the limit of a slightly rough surface and the model for microrough surfaces might be appropriate to use for the reflectance determination. This can be explained via physical grounds because the ratio λ/σ determines the resulting directional distribution. For $\lambda/\sigma \gg 1$ the surface will appear smooth and a strong reflected component and a weak nonspecular component (diffuse) will occur, which is a similar trend that occurs in the limit of slightly rough surface reflectors. As expressed

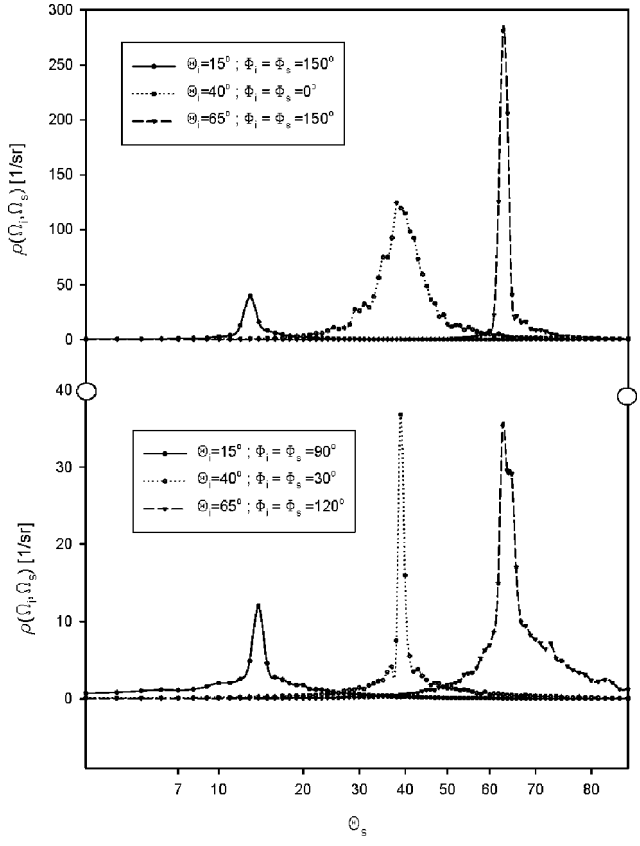

Fig. 5 Off-specular shifting (apparent) in the reflectance function for aluminum and stainless-steel 321 foils for various angles of incidence ($\lambda = 0.633\ \mu$m).

in Eq. (4), the PSD of the surfaces must be determined before calculating the reflectance function.

There are several ways to determine the PSD of a surface. Some profilometers are able to obtain the one-dimensional PSD up to a three-dimensional map of the surface. Due to availability, it was decided to use an atomic force microscope (AFM) to map the metallic surfaces. Atomic force microscopy is capable of measuring the profile of the exposed surface of a material. The two-dimensional PSD can be obtained from these measurements because it is simply the square of the magnitude of the Fourier transform of the surface height function.

A multimode AFM, Model MMAFM-153, was utilized to perform surface characterization and to obtain the isotropic two-dimensional PSD for the foils. Different scan rates and spatial frequencies for the surface characterization had to be used because of the fact that the nanoprobe would tend to "jump" drastically while encountering some rough parts. (PSD is utilized as a metrological tool for evaluating extremely flat surfaces, something not accomplished with the foils.) Due to the nature of these rough surfaces (fractal surface finish) the PSD also diverges and grows at low frequencies as pointed out before. Similarly, the values of the rms roughness,

$$\sigma = \int_0^\infty f df_x S_2(x)$$

and the autocorrelation length,

$$lc = \frac{1}{2\sigma^4} \int_0^\infty df_x S_2(x)$$

obtained by the AFM were inaccurate and erratic in comparison with the values obtained via the stylus technique. Also, due to the anisotropy and roughness of the materials (Fig. 6), which clearly shows the rugged or brushed surface appearance of the aluminum

Table 2 S_4 hemispherical positions

Port	θ, deg	ϕ, deg
1	73	18
2	73	342
3	73	288
4	73	252
5	73	198
6	73	162
7	73	108
8	73	72
9	25	45
10	25	135
11	25	225
12	25	315

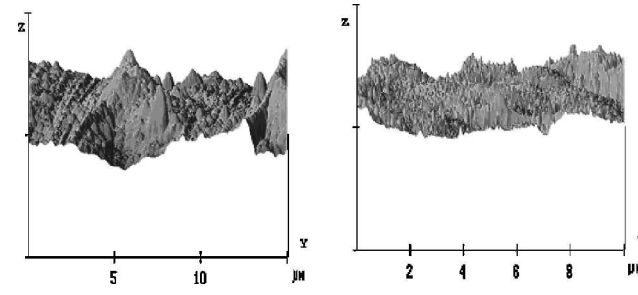

Fig. 6 Three-dimensional surface profile of aluminum foil (left) and stainless-steel foil (right): scan size, 15 um; scan rate, 0.5003 Hz; number of samples, 256.

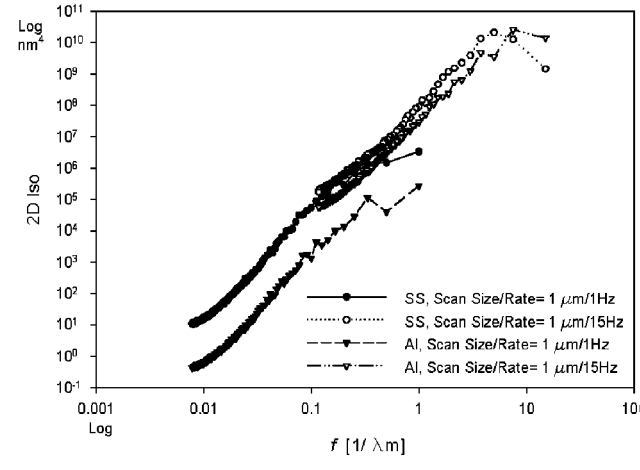

Fig. 7 The isotropic two-dimensional power spectral density (SS 321 and aluminum foils for various scan sizes and rates).

foil in comparison with the smoothness of the stainless-steel foil, the PSD extracted from the AFM (Fig. 7) proved to be inconclusive and unreliable because different PSD values were obtained for the same sample and scan rate, which in turn might lead to nonunique reflectance data.

The preceding procedures yielded inconclusive prediction of reflection data. It has been noted that experimentation can provide accurate reflection function data to be used or analyzed in radiative transfer calculations. By using a simple prototype hemispherical optical scattering instrument based on the discrete ordinate method (DOM),[21] the reflectance data obtained from this device can be directly applied to an S_4 scheme code (for boundary conditions) when solving the radiative transfer equation. Table 2 shows the S_4 directional positions.

To provide the input intensity power, three different types of infrared sources (Ion Optics®) that work separately depending on the wavelength range were used for the experimentation. Two windowless broad infrared light sources provided power for a wavelength range from 2 to 20 μm, ReflectIR-P1N and TO-5. The former is

a collimated source whereas the latter has a broad normalized output pattern. The third light source is a collimated light source with a range in wavelength from 2 to 5.25 μm (ReflectIR-P1S) with a normalized output pattern similar to the other collimated source.

According to the ASTM designation E-1392-90,[19] the reflectance function can be measured and normalized using four types of normalizations. It is the choice in this work to normalize the scattered power to the incident power in a relative manner (except for the NIST measurements, which were normalized in an absolute manner). This relative technique normalizes the sample data to that of a reference standard or highly reflectant diffuse surface[19] with a known spectral reflectance function.

Due to the fact that the working wavelength region is between the near infrared to midinfrared, an Infragold® diffuse reflectance standard, from Labsphere, Inc., was selected. It is a typical material with a high hemispherical reflectance value for this spectral region and provides sufficient energy levels over the entire range of incident angles.

Despite the fact that the calibration from 2.5 to 15 μm every 50 nm is traceable to the current NIST standards, the reflectance function for the Infragold had to be measured due to the type of infrared sources used during the experiments. Figures 8 and 9 show the normalized reflectance function for the reflectance standard for different types of source. Out-of-plane measurements for this material yield small values of reflectance similar to one another, which agrees well with the calibration. Figure 9 also shows a peculiarity of this lambertian surface. When the incident angle is located at the bottom of the scatterometer there are always peaks in the reflectance function. One of them constitutes the specular peak and the other is located at the upper angles. This phenomenon might be produced by multiple scattering reflections in the surface for such grazing angles.

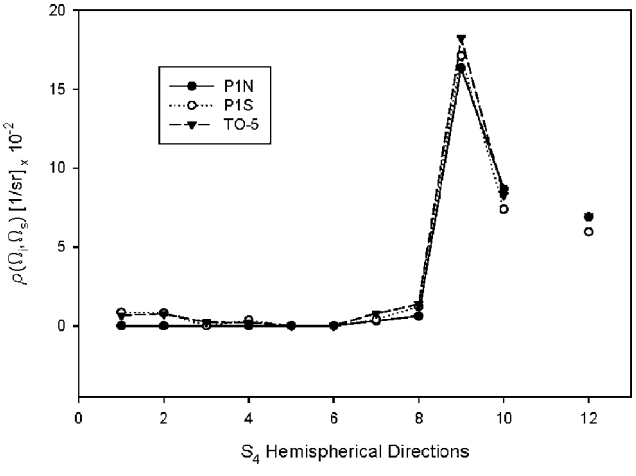

Fig. 8 Reflectance of Infragold using various light sources with incident angle of Θ = 25 deg, Φ = 225 deg.

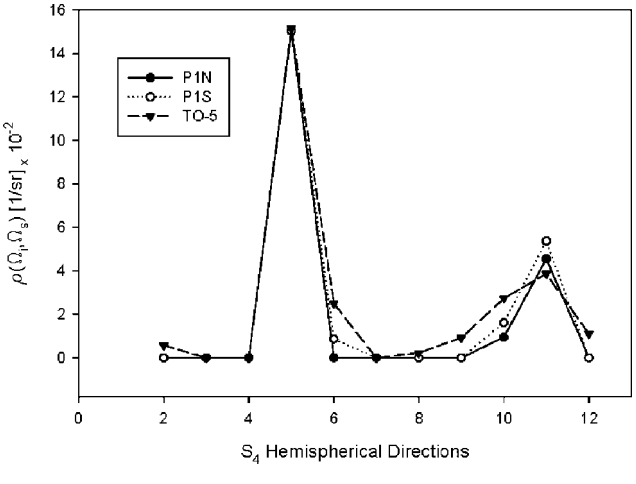

Fig. 9 Reflectance as a function of the detector number of aluminum foil using various light sources with incident angle of Θ = 73 deg, Φ = 18 deg.

A. Uncertainty

Because the reflectance function is obtained through the ratio of voltage signals, there is great reduction in the overall uncertainty of the experiment. However, the contributions to this value, after following the guidelines from Kim et al.,[22] can be stated as follows.

The sample materials to be analyzed as previously described are the aluminum foil and the 321 stainless steel. Both metallic surfaces were carefully attached to the blackened holders and properly cleaned before sampling. Ensuring complete flatness of all samples was not possible, which can have an effect on the measured reflectance values. Due to the machining process of the hemispherical scatterometer, the scattering or receiving angles have an average deviation of ±0.25 deg (±0.005 radians) with respect to the exact values of the S_4 approximation. The contribution of this angular uncertainty and the solid angle uncertainty can be considered small because each detector has the same solid angle, and a large hole aperture guarantees that the field of view of the detector includes the entire sample irradiated area.

In addition to incident energy measurement, source and detector output variations (amplifier) and external setup components compose the overall system bias of the approximately 6.0%.

To ensure more accurate and less noisy signals through the detectors, the signals were recorded using Wavestart®, a software package that connected the oscilloscope with the personal computer. By using a Gaussian filtering approach the signals were denoised to obtain a smooth reading without losing the inherent details of the main signal. An average of 1400 data points per sample was collected through the oscilloscope acquisition for each detector to guarantee uniformity of the signals.

The use of the reference standard can also be a factor that increments the uncertainty of the data. Bias of the signals was calculated for each one of the obtained readings. Combining all the preceding factors in addition to the noise that emanated from the detectors, the statistical measurement uncertainty was calculated at 4.2%.

Using $U_q = \sqrt{(P_q^2 + B_q^2)}$, where P_q is the contribution to the uncertainty and B_q is a bias contribution, the combined uncertainty is approximately ±7.39%.

Moreover, in order to reverify that the measured reflectance function values are correct, the hemispherical reflectance of the Infragold is calculated using the unnormalized measured data. All of this unnormalized data of the reflectance function are divided by the cosine of the incident polar angle Θ_i. The hemispherical reflectance is defined as the fraction of the total irradiation from all directions reflected into all directions[2] and is expressed as

$$\rho = \frac{\int_{2\pi}\int_{2\pi} \rho(\Omega_i \Omega_s)\cos(\Theta_s) I(r, \Omega_i)\cos(\Theta_i)\,\mathrm{d}\Omega_s\,\mathrm{d}\Omega_i}{\int_{2\pi} I(r, \Omega_i)\cos(\Theta_i)\,\mathrm{d}\Omega_i} \tag{6}$$

where $\rho(\Omega_i \Omega_s)$ is the reflectance function and $I(r, \Omega_i)$ is the incident intensity per established direction. However, Eq. (6) is not directly suitable for the measurements taken by the DOM scatterometer because it involves directional intensity effects.

A method of integrating the diffuse part of all the reflectance functions produced by the 12 different intensities and adding the weighted summation of all the specular components produced by the 12 different intensities should lead to a calculated value comparable to the calibrated hemispherical reflectance. Thus,

$$\rho(r) = \sum_{j=1}^{N}\sum_{i=1}^{N} w_j w_i \rho^d(r, \Omega_i, \Omega_s)\cos(\Omega_s)$$

$$+ \frac{1}{\pi}\sum_{i=1}^{N} w_i \frac{\rho^s(r, \Omega_i, \Omega_s)}{\cos(\Omega_i)} \tag{7}$$

where N represents the number of incident directions, ρ^d is the weak diffuse part of the reflectance function, and ρ^s the strong

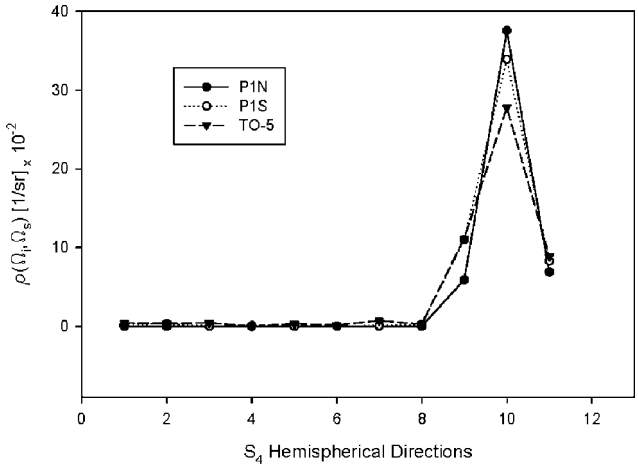

Fig. 10 Reflectance as a function of the detector number of aluminum foil using various light sources with incident angle of Θ = 25 deg, Φ = 315 deg.

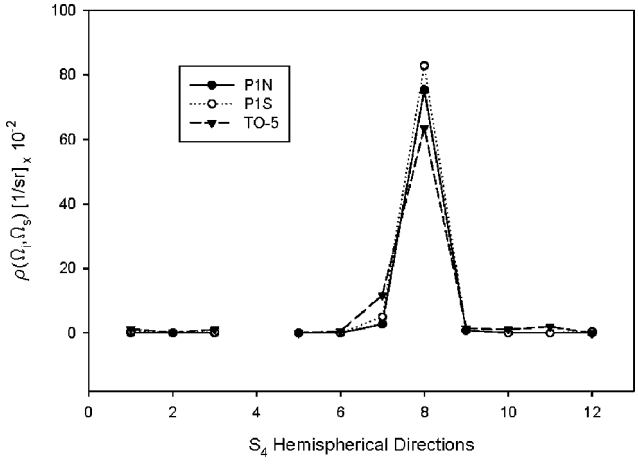

Fig. 11 Reflectance as a function of the detector number of aluminum foil using various light sources with incident angle of Θ = 73 deg, Φ = 252 deg.

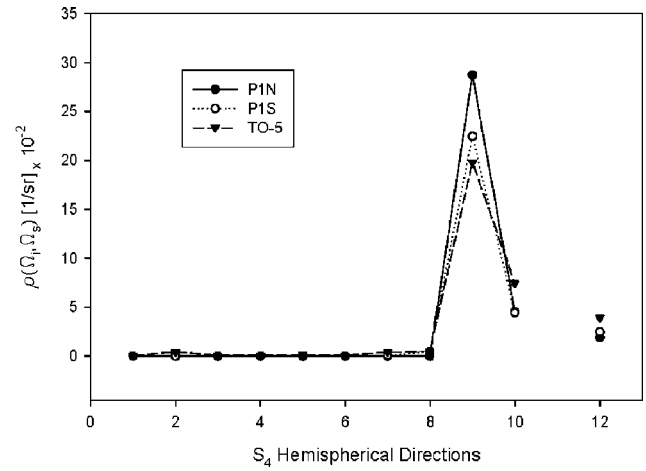

Fig. 12 Reflectance as a function of the detector number of stainless-steel foil using various light sources with incident angle of Θ = 25 deg, Φ = 225 deg.

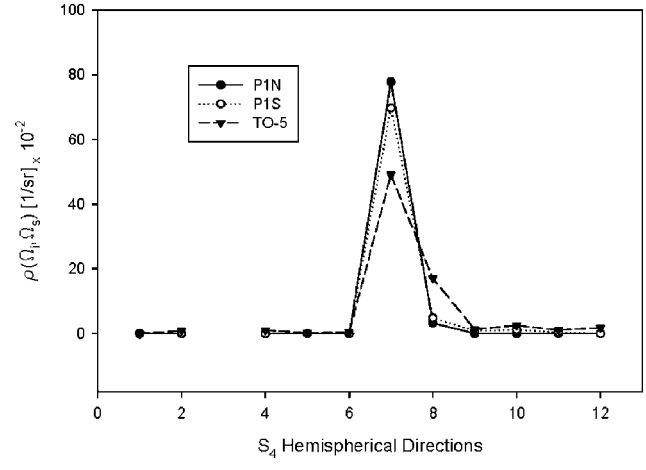

Fig. 13 Reflectance as a function of the detector number of stainless-steel foil using various light sources with incident angle of Θ = 73 deg, Φ = 288 deg.

specular component of the function. By solving Eq. (7) using the DOM integration method and an S_4 equal weight quadrature,[2] the calculated hemispherical reflectance of Infragold was 0.975, a 1.2% error with the average calibrated hemispherical reflectance provided by the manufacturer.

B. Aluminum

Figures 10 and 11 show the experimental data for the reflection function for different incident positions and different light sources. It is noted that due to the random distribution of the surface material, the reflectance is slightly different for opposite specular positions. This trend is similar for the rest incident position angles. The data also unveil a slight difference in reflection between the two wavelength ranges. This difference is likely due to the fact that at longer wavelengths the surfaces tend to behave more specularly. Illuminating the sample with an uncollimated source does not provide sufficient evidence of surface description.

C. Stainless Steel

As pointed out previously for the aluminum sample, the data obtained for the less rough steel foil follows the same trends with respect to the port positions. For this particular case, the angle positions of the quadrate indicate different trends in reflectance function. Because this material is less rough than the aluminum foil, the specular reflection effects depending on the wavelength range are more noticeable than for the aluminum foil. The data obtained for the 2–20-μm range are slightly higher than those for the range from 2 to 5.25 μm, which agrees qualitatively with the literature.[10,11] Also, the reflectance function obtained for angles of incidence for the upper positions of the S_4 quadrature are much lower than the respective reflectance function values of the mirrorlike aluminum foil for the same positions. The inverse trend happens for the lower incident position angles because, at these bigger incident polar angles, the surfaces tend to reach a specular behavior. That is, the smoother the surface is, the bigger the reflection obtained, as shown in Figs. 12 and 13 in comparison with Figs. 10 and 11.

IV. Conclusions

The reflectance function of any surface is dependant on several parameters; among them are the rms surface roughness, incident energy wavelength, and directions.

Because, for the cases considered, the surface is rougher than permitted by the smooth-surface requirement, the PSD of the surface peaks at small frequencies, as some fractal surfaces cannot be extrapolated to another frequency. Furthermore, some nonexistent PSD values at certain frequencies can appear in the peridogram, which leads to the use of a different, more complete, theory requiring numerical evaluation.

Another possible complication comes from the fact that some of the analytical methods take the surface to be an infinite half-space of homogeneous material rather than, say, a layered structure without considering subsurface complications. The result is that the actual measurement of the reflectance function is the best way to

determine this radiative property and to measure it in such manner that could also be applied to general participating radiation heat transfer solutions.

These results provide a simplified measure of scattering data for surface and pattern recognition and can be used as a reference tool for machining and surface finish processes using grayscale data because a reflection pattern can be established and, through the use of recognition tools such as neural networks, quality of the materials after machining processes can be further reassured.

Measuring the reflectance data at each of the 12 port positions produced an enormous amount of data that can be easily classified and retrieved as a reference tool for later use in any specific industrial, research, and academic investigations.

By the use of the scatterometer, the manner in which a mirror-like surface behaved at different incident angles with respect to a much smoother one for the same incident angles was discovered. All metallic samples comprising the fire barrier show a similar trend, which guarantees the uniformity of the data. Using the collimated light sources it was possible to assess a position that produced the highest specular reflection.

Acknowledgments

A great deal of thanks is extended to all people who collaborated in some technical details during the research leading to this work. Especially we thank Tom J. Love Jr., Eugene Church, and Thomas Germer at the NIST for their contribution and guidance in the reflectance function determination; Jayaraman Raja at the University of North Carolina, Charlotte, North Carolina, for the metrology measurements; and Edgar A. O'Rear III for allowing the use of the AFM.

References

[1]Love, T. J., *Radiative Heat Transfer*, Merrill, Columbus, OH, 1968, pp. 38–45.

[2]Modest, M. F., *Radiative Heat Transfer*, McGraw–Hill, New York, 1993, pp. 84–89, 542–547.

[3]Stover, J. C., *Optical Scattering, Measurement and Analysis*, 2nd ed., SPIE Optical Engineering Press, Bellingham, WA, 1995, pp. 19–27.

[4]Tang, K., Dimenna, R. A., and Buckius, R. O., "Regions of Validity of the Geometric Optics Approximation for Angular Scattering from Very Rough Surfaces," *International Journal of Heat and Mass Transfer*, Vol. 40, No. 1, 1997, pp. 49–59.

[5]Church, E. L., Tacks, P. Z., and Leonard, T. A., "Prediction of BRDFs from Surface Profile Measurements," *Scatter from Optical Components*, edited by J. C. Stover, Proceedings of the Society of Photo-Optical Instrumentation Engineers, Vol. 1165, Society of Photo-Optical Instrumentation Engineers, Bellingham, WA, 1990, pp. 136–150.

[6]Davies, H., "The Reflection of Electromagnetic Waves from a Rough Surface," *Proceedings of the Institution of Electrical Engineers*, Vol. 101, No. 4, 1954, pp. 209–214.

[7]Bennet, H. E., and Porteous, J. O., "Relation Between Surface Roughness and Specular Reflectance at Normal Incidence," *Journal of the Optical Society of America*, Vol. 51, No. 2, 1961, pp. 123–129.

[8]Beckmann, P., and Spizzinno, A., *The Scattering of Electromagnetic Waves from Rough Surfaces*, Pergamon, New York, 1963, pp. 110–124, Chap. 2.

[9]Birkeback, R. C., and Eckert, E. R. G., "Effects of Roughness of Metal Surfaces on Angular Distribution of Monochromatic Reflected Radiation," *Journal of Heat Transfer*, Vol. 87C, Feb. 1965, pp. 65–94.

[10]Torrance, K. E., and Sparrow, E. M., "Theory for Off-Specular Reflection from Roughened Surfaces," *Journal of the Optical Society of America*, Vol. 9, No. 9, 1967, pp. 1105–1111.

[11]Love, T. J., and Francis, R. E., "Experimental Determination of Reflectance Functions for Type 302 Stainless Steel," *Thermophysics of Spacecraft and Planetary Bodies*, edited by G. Heller, Academic Press, New York, 1967, pp. 90–106.

[12]Smith, A. M., Muller, P. R., Frost, W., and Hsia, H. M., "Super- and Subspecular Maxima in the Angular Distribution of Polarized Radiation Reflected from Roughened Dielectric Surfaces," *Heat Transfer and Spacecraft Thermal Control*, edited by J. W. Lucas, MIT Press, Cambridge, MA, 1971, pp. 249–269.

[13]Houchens, A. F., and Hering, R. G., "Bidirectional Reflectance of Rough Metal Surfaces," *Thermophysics of Spacecraft and Planetary Bodies*, edited by G. B. Heller, Academic Press, New Orleans, LA, 1967, pp. 65–89.

[14]Cohn, D. W., Tang, K., and Buckius, R. O., "Comparison of Theory and Experiments for Reflection from Microcontoured Surfaces," *International Journal of Heat and Mass Transfer*, Vol. 40, No. 13, 1997, pp. 3223–3235.

[15]Germer, T. A., "Multidetector Hemispherical Polarized Light Scattering Instrument," *Rough Surface Scattering and Contamination*, edited by P. T. Chen, Z. H. Gu, and A. A. Maradudin, Vol. 3784, SPIE Optical Engineering Press, Bellingham, WA, 1999, pp. 296–303.

[16]Germer, T. A., "Polarized Light Scattering by Microroughness and Small Defects in Dielectric Layers," *Journal of the Optical Society of America A*, Vol. 18, No. 6, 2001, pp. 1279–1288.

[17]Marschner, S. R., Westin, S. H., Lafortune, E. P. F., and Torrance, K. E., "Image-Based BRDF Measurement," *Applied Optics*, Vol. 36, No. 16, 2000, pp. 2592–2600.

[18]Caplinger, G. D., Sutton, W. H., Spindler, R., and Golke, H., "Transient Heat Transfer for Layered Ceramic Insulation and Stainless Steel Foil Fire Barriers," *Journal of Heat Transfer*, Vol. 121, 1999, pp. 1059–1066.

[19]"Standard Practice for Angle Resolved Optical Scatter Measurements on Specular or Diffuse Surfaces," ASTM Standard E1392-90, American Society for Testing and Materials, Philadelphia, 1990.

[20]"Surface Texture (Surface Roughness, Waviness and Lay)," ANSI/ASME B46.1, American National Standards Inst., New York, 1990.

[21]Sanchez, M. A., "A Study of Directional Radiative Properties of Thermal Fire Barriers," Ph.D. Dissertation, School of Aerospace and Mechanical Engineering, Univ. of Oklahoma, Norman, OK, 2002.

[22]Kim, J. H., and Simon, T. W., "Journal of Heat Transfer Policy Following on Reporting Uncertainties in Experimental Measurements and Results," *Journal of Heat Transfer*, Vol. 15, Feb. 1993, pp. 5, 6.